The current issue and full text archive of this journal is available at
www.emeraldinsight.com/0332-1649.htm

An aid for teaching hybrid propulsion systems with emphasis on their electric drive unit

Asma Ben Rhouma and Ahmed Masmoudi
Research Unit on Renewable Energies and Electric Vehicles (RELEV), University of Sfax, Sfax, Tunisia

Abstract

Purpose – The purpose of this paper is to propose an approach to teach to post-graduate students the basis of hybrid propulsion systems (HPS) with emphasis on their electric drive unit.

Design/methodology/approach – Following the introduction of the basic topologies of HPS, a case study is focused with an analysis of its current features. Of particular interest, those related to the flux-weakening range extension and the cost-effectiveness improvement are rethought in an attempt to stimulate the innovative capabilities of the students.

Findings – The adopted methodology has been integrated in a master course and has been found attractive and informative by the students.

Practical implications – The proposed teaching approach should be complemented by appropriate laboratory courses.

Originality/value – Thanks to the proposed methodology, the basis of HPS is no longer restricted to a selected population of the electrical engineering community.

Keywords Electromagnetism, Electric machines, Flux, Cost effectiveness, Electric power systems, Automotive industry

Paper type Research paper

1. Introduction

Until the 1960s, automotive manufacturers did not worry about the cost of fuel. They had never heard of air pollution, and they never thought about life cycle. Ease of operation with reduced maintenance costs meant everything back then. Nowadays, clean air mandates are driving the market to embrace new propulsion systems built around an internal combustion engine (ICE) and an electric motor, yielding the so-called hybrid propulsion systems (HPS).

HPS are currently regarded as viable candidates for the substitution of ICE-based propulsion systems (Boldea, 2010; Miller, 2006; Toyota, 2003). They offer a sustainable mobility with a great improvement of the quality of life in highly populated cities. Within this universal trend, the automotive market is continuously supplied by new hybrid vehicles. Some of them are already popular worldwide.

Besides the automotive industry, many research teams worldwide are deeply involved in R&D projects focused towards the design of efficient, cost-effective, compact

The works developed within the project "Delta-inverter-fed brushless DC motor drives" were supported by Allison Transmission Division of General Motors, Indianapolis, Indiana, USA.

COMPEL: The International Journal for Computation and Mathematics in Electrical and Electronic Engineering
Vol. 30 No. 1, 2011
pp. 374-391

0332-1649
DOI 10.1108/03321641111091610

and reliable HPS. Of particular interest is the electric drive unit (EDU) whose feature optimization and traction capabilities are the subject of intensive investigations.

Until recently, electrical machines have been designed assuming that they will be connected to an infinite bus. This has led to the well-known conventional AC machines (induction and wound field synchronous machines) in which the stator windings are sinusoidally distributed in slots around the air gap so as to couple optimally with the sinusoidal supply. The significant advances in the power electronic converter technology have removed the need of such a concept as the basis for machine design. Consequently, a novel era of electric machine technology has been evolving, based on the principle that the best machine design is the one that simply produces the optimum match between the machine and the power electronic converter, yielding the so-called "converter fed machines" (CFMs). Within this trend, much attention is presently paid in the design of new topologies of CFMs where many conventional considerations are rethought, such as the number of phases, the number of poles, the winding shape and distribution, the magnetic circuit material and geometry, radial, axial or circumferential path and so on (Zhu, 2009; Ben Hamadou *et al.*, 2009; Tajima *et al.*, 2002).

In the manner of the electric machines, the associated converters are continuously the subject of optimization. The most important optimization criteria in the field of HPS are:

- the cost-effectiveness;
- the compactness; and
- the reliability.

These could be gained thanks to reduced-structure inverters (Elantably *et al.*, 2010; Ben Rhouma and Masmoudi, 2008; El Badsi and Masmoudi, 2008; Ben Rhouma *et al.*, 2007; Lee *et al.*, 2003).

Accounting for the emergence of HPS, it turns to be vital to schedule, for a long term, a public education policy of this evolving technology. To put into practice, such a policy, and as a short-term approach, HPS should be included, at different levels, of the electrical and electro-mechanical engineering education programs. Within this commitment, the paper proposes an aid for teaching the basis of HPS to post graduate students, as well as an approach to stimulate their innovative capabilities, considering the Toyota Prius as a case study.

2. HPS: a brief review

2.1 Background

There is currently a revolution under way in the total scope of automotive technology. The immediate emphasis is on exploiting developments in propulsion system technology. While economists bemoan the resource impacts associated with fossil fuel, and environmentalists demonstrate against the evils of air pollution, politicians under pressures from these groups constantly advertise their efforts to save the world from vehicular fuel pollution. These factors have cumulatively exerted enormous pressures on the automotive industry to satisfy the activists and placate the politicians.

Some emergent technologies that offer solutions to the above-cited problems, have been already manufactured, others are under investigation. The ICE, which has reigned supreme for more than 100 years, still has room for improvement. Diesels now deliver economy, sophistication and power that could only be dreamed of ten years ago. The most immediate prospect from among the emergent technologies for a dramatic

advance in the state of the art for fuel economy and emission control is based on the concept of a conventional ICE boosted by an electric motor as a second propeller. Such a concept is termed as "hybrid propulsion system".

2.2 HPS: basic topologies

Referring to the published material and to the manufactured concepts, one can classify the HPS into three major categories:

(1) the series hybrid;

(2) the parallel hybrid; and

(3) the series/parallel hybrid.

2.2.1 Series HPS. The bloc diagram of the powertrain of a series HPS is shown in Figure 1.

Operated at almost steady-state around its rated point, the engine (ICE) drives the generator that feeds the electric motor solely acting as propeller. The power bidirectionally flows in the battery pack:

- into from the ICE during recharging or from the motor during regenerative breaking; and
- out to the motor during startup and extra power demand.

2.2.2 Parallel HPS. The bloc diagram of the powertrain of a parallel HPS is shown in Figure 2.

Both the ICE and the electric motor drive the wheels with appropriate power ratios. The battery pack is recharged by switching the motor to act as a generator. In spite of its simplicity, the parallel HPS cannot drive the wheels from the electric motor while simultaneously charging the battery pack.

2.2.3 Series/parallel HPS. The bloc diagram of the powertrain of a series/parallel HPS is shown in Figure 3.

It combines the features of the series and the parallel hybrid systems in an attempt to maximize the benefits of both systems. Depending on the driving conditions, the series/parallel HPS uses only the motor as a propeller or both the motor and the ICE, in an

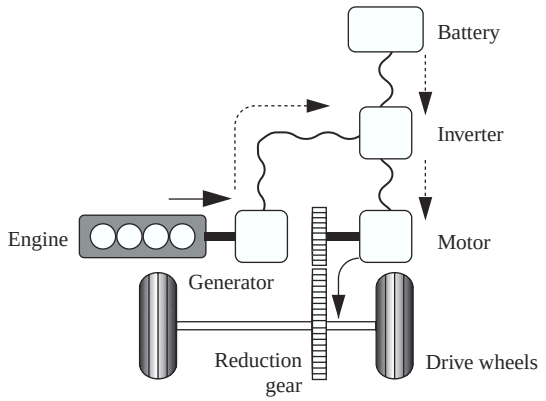

Figure 1.
Bloc diagram of the powertrain of the series HPS

Source: Toyota (2003)

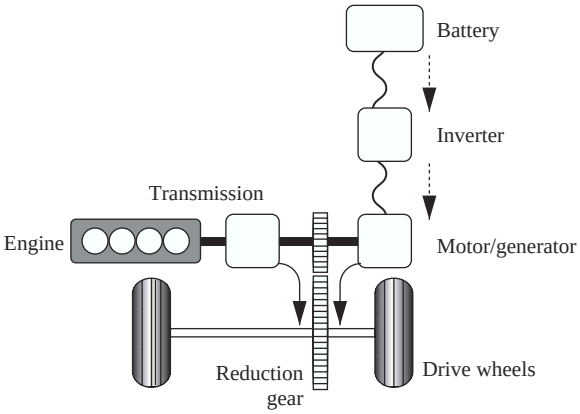

Source: Toyota (2003)

Figure 2.
Bloc diagram of the powertrain of the parallel HPS

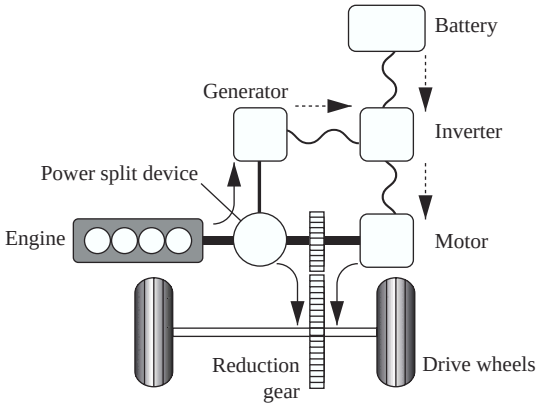

Source: Toyota (2003)

Figure 3.
Bloc diagram of the powertrain of the series/parallel HPS

attempt to access efficient operating cycles. This is achieved thanks to the power-split device. A detailed description of this system and of its operating cycles is provided in the following section.

2.3 Case study

This section is aimed at the description and the operating cycles of the HPS of the Toyota Prius. Such a choice is far of being arbitrary, in so far as up to date, the Toyota Prius is the most popular hybrid vehicle worldwide. The Toyota Prius is equipped by a series/parallel HPS.

2.3.1 Description of the series/parallel HPS of the Toyota Prius. The HPS of the Toyota Prius is built around two power sources (Toyota, 2003):

(1) a gasoline engine using the Atkinson cycle; and

(2) a brushless synchronous motor with V-shaped permanent magnets (PMs) in the rotor.

It also includes (Toyota, 2003):

- a generator which behaves as a starter-alternator;
- a nickel-metal (Ni-MH) battery pack, made up of 168 cells providing a DC voltage $U_B = 201.6$ VDC; and
- a static converter including an inverter connected to the motor and a voltage booster enabling an increase of the battery voltage from U_B to $U_{DC} = 500$ V at the input of the inverter.

Depending on the driving conditions, the Toyota Prius HPS uses only the motor as a propeller or both the motor and the engine, in an attempt to access efficient operating cycles with reduced emissions of green house gases. This is achieved, thanks to the power split device. Furthermore, and when required, a boost of power, pulled from the battery pack, is applied to the motor in order to achieve accelerations at mid- to full-range speeds. Finally and under certain circumstances, the generator produces electricity to replenish the battery pack.

The bloc diagram of the powertrain of the HPS of the Toyota Prius is shown in Figure 4.

2.3.2 Operating cycles. Referring to Toyota (2003), the Prius series/parallel HPS is managed within five major operating cycles which are described as follows:

- *Cycle 1: start-up and low- to mid-range speeds*. The vehicle is propelled by the electric motor fed exclusively by the battery puck. This strategy represents a crucial ecological benefit as far as the high emission of green house gases, which penalizes the engine, is discarded.
- *Cycle 2: mid- to full-range speeds in normal drive*. The engine provides the propulsion power which is divided by the power-split device. A part drives the generator, which in turn drives the motor. The remaining part of the engine power is directly applied to the wheels. The power allocation is controlled to maximize the hybrid system efficiency.

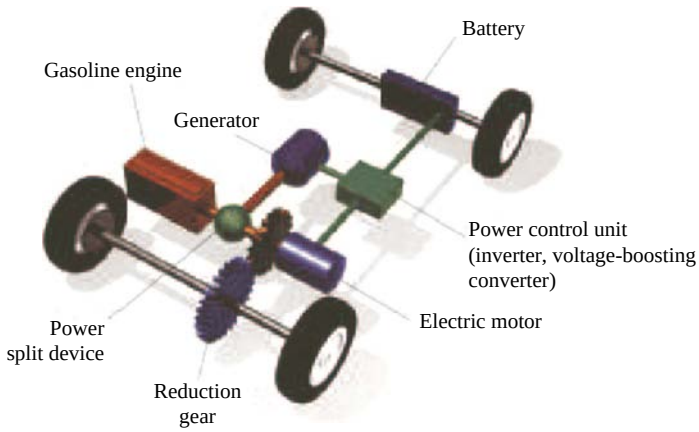

Source: Toyota (2003)

Figure 4.
Bloc diagram of the series/parallel HPS of the Toyota Prius

- *Cycle 3: mid- to full-range speeds with acceleration.* Beyond the scenario of the second cycle, the motor is fed by an extra power provided by the battery pack. Such an increase of the propulsion power is required under some circumstances, for instance during climbing a slope.
- *Cycle 4: deceleration and braking.* During deceleration and braking, the engine is systematically stopped while the electric motor and the associated inverter turn to be a generator and a rectifier, respectively. These enable the conversion of the wheel kinetic energy into electrical energy, which is stored in the battery pack, leading to the so-called regenerative braking. This operating cycle offers a crucial efficiency benefit compared to the conventional braking systems.
- *Cycle 5: battery pack recharging.* The engine drives the generator to recharge the battery pack when necessary. It should be noted that charging the battery pack could be carried out under no-propulsion operation or could be combined with cycles 2 and 4.

The above-described operating cycles are shown in Figure 5.

3. Flux-weakening range: investigation and extension

Considering the Toyota Prius as a case study, this section is dedicated to:

- an initiation of the students to the investigation of the electric motor features related to the flux-weakening range, assuming smooth poles in the rotor and negligible resistances in the armature; and
- a stimulation of the innovative potentialities of the students, through the proposal of a solution to extend the flux-weakening range.

3.1 Flux-weakening range investigation

3.1.1 Determination of the rated flux ratio. Let us consider the expression of the rated flux ratio ρ_r, such that:

$$\rho_r = \frac{LI_r}{\Phi_{pm}} \tag{1}$$

where L and I_r are the armature inductance and rated current, respectively, and Φ_{pm} is the PM flux.

The armature fed by its rated current under zero angular shift from the phase-back electromotive force (EMF), one can express the base speed Ω_b and the maximum speed Ω_{max} in terms of ρ_r as follows:

$$\begin{cases} \Omega_b = \frac{V_{max}}{P\Phi_{pm}\sqrt{1+\rho_r^2}} \\ \Omega_{max} = \frac{V_{max}}{P\Phi_{pm}(1-\rho_r)} \end{cases} \tag{2}$$

Then, the ratio $\Gamma = (\Omega_{max}/\Omega_b)^2$ is deduced from equation (2) as follows:

$$\Gamma = \frac{1+\rho_r^2}{(1-\rho_r)^2} \tag{3}$$

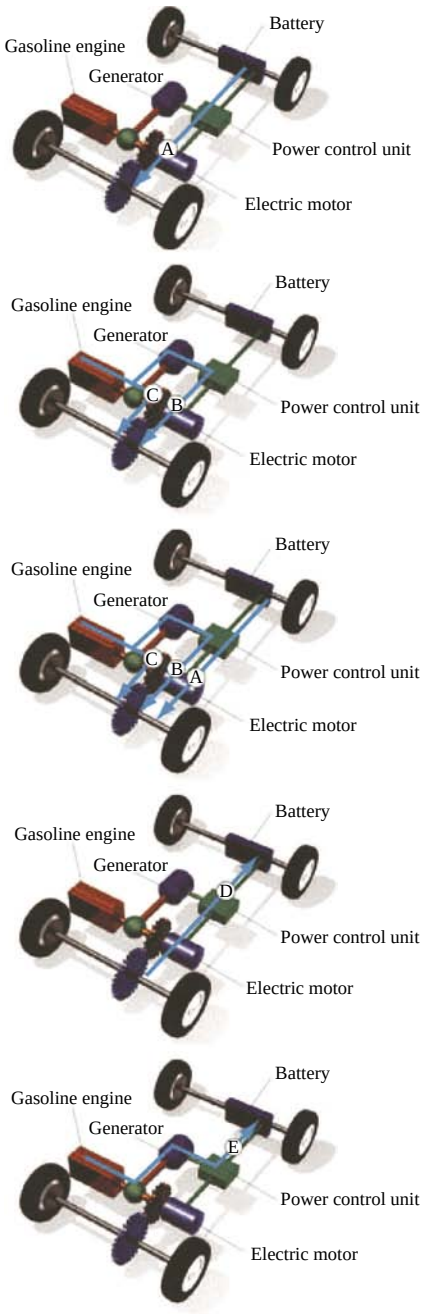

Cycle 1: Start-up and low- to mid-range speeds

Cycle 2: Mid- to full-range speeds in normal drive

Cycle 3: Mid- to full-range speeds with acceleration

Cycle 4: Deceleration and braking

Cycle 5: Battery pack recharging

Figure 5.
Major operating cycles of the HPS of the Toyota Prius

Source: Toyota (2003)

Accounting for the data provided in Section 2.3.1, the resolution of equation (3) gives $\rho_r = 0.75$.

3.1.2 Determination of the armature inductance. The determination of L is carried out following three steps. First, the PM flux Φ_{pm} is found out:

$$\Phi_{pm} = \frac{V_{max}}{P\Omega_{max}(1-\rho_n)} \simeq 716\,\text{mW} \tag{4}$$

Then, the rated armature current is deduced from the rated electromagnetic torque T^r_{em}, such that:

$$I_r = \frac{3P\Phi_{pm}}{T^r_{em}} \simeq 93\,\text{A} \tag{5}$$

Finally, the armature inductance is determined using the expression of the rated flux ratio, as follows:

$$L = \frac{\rho_n \Phi_{pm}}{I_r} \simeq 5.77\,\text{mH} \tag{6}$$

3.1.3 Determination of the power factor at the base speed. Omitting the armature resistance, the electromagnetic power P_{em} turns to be equal to the armature absorbed power P_a which, for the base speed, is expressed as follows:

$$P^r_{em} = T^r_{em}\Omega_b = P^r_a = 3V_{max}I_r cos\varphi_b \tag{7}$$

where $cos\varphi_b$ is the power factor at Ω_b which is find out by substituting T^r_{em} in equation (7), as:

$$cos\varphi_b = \frac{P\Phi_{pm}\Omega_b}{V_{max}} = 0.8 \tag{8}$$

3.2 A proposal to extend the flux-weakening range

Referring to El-Refaie and Jahns (2005) and El-Refaie *et al.* (2006), this could be achieved through the substitution of the armature distributed windings by concentrated ones. Indeed, it has been established that concentrated windings make it possible to significantly increase the machine inductance in order to reduce the characteristic current to the point of establishing equality with the rated current. This offers the possibility of optimal flux weakening for which the flux ratio ρ turns to be equal to unity and the maximum speed Ω_{max} tends to infinity. In order to confirm this statement, Figure 6 shows the flux-weakening range width to the basic speed ratio versus the flux ratio.

Concentrated windings exhibit further interesting features, such as:

- their short end-winding leading to reduced copper losses and improved compactness, especially when double-layer slots are considered (Zhu, 2009);
- their high slot fill factors especially when coupled to segmented stator structures (Zhu, 2009);
- their interesting fault-tolerance capabilities thanks to their low mutual inductances, especially when single-layer slots are considered (Bianchi *et al.*, 2005); and
- their low-intrinsic cogging torque (Bianchi and Bolognani, 2002).

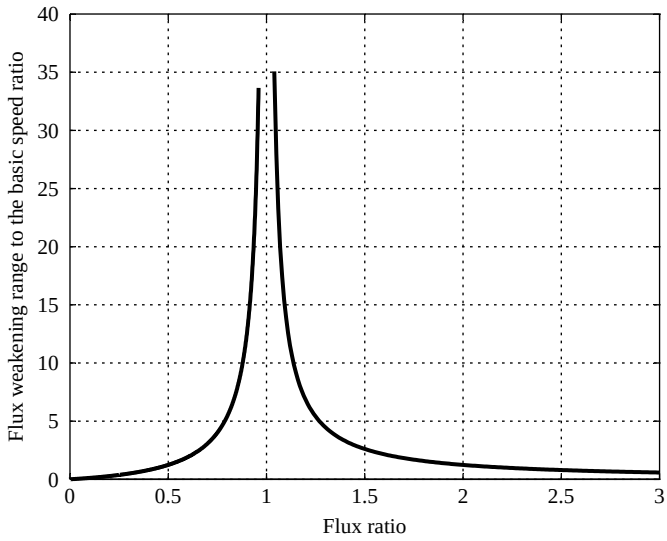

Figure 6.
Flux weakening range width to the basic speed ratio versus the flux ratio

This said, it is to be noted that these advantages could not be accessed without a suitable selection of the slot/pole combination (Zhu, 2009; Ben Hamadou *et al.*, 2009).

In what follows are investigated the motor parameters and features, foreseen in the case of optimal flux-weakening operation.

3.2.1 Determination of the armature inductance for infinite flux-weakening range. Assuming that the rated armature current and electromagnetic torque are the same as those of the real design of the PM motor, one can find out the armature inductance L_∞ under optimal flux-weakening operation. To do so, let us express the corresponding flux ratio ρ_∞, as follows:

$$\rho_\infty = \frac{L_\infty I_r}{\Phi} = 1 \tag{9}$$

which leads to:

$$L_\infty \simeq 7.7\,\text{mH}$$

3.2.2 Determination of the electromagnetic power in the flux-weakening range. The electromagnetic power $P_{em\infty}$ turns to be constant in the whole flux-weakening range starting from the base speed $\Omega_{b\infty}$. Therefore, $P_{em\infty}$ could be determined considering the rated speed which is reduced to:

$$\Omega_{b\infty} = \frac{V_{max}}{\sqrt{2}P\Phi} \simeq 1,061\,\text{rpm} \tag{10}$$

then:

$$P_{em\infty} = \Omega_{b\infty} T^r_{em} \tag{11}$$

which gives:

$$P_{em\infty} \simeq 44.4\,\text{kW}$$

3.2.3 Determination of the power factor at the base speed. The application of equation (8) in the case of an infinite flux-weakening range, gives:

$$\cos\varphi_{b\infty} = \frac{P\Phi\Omega_{b\infty}}{V_{max}} \tag{12}$$

Accounting for the expression of $\Omega_{b\infty}$ given in equation (10), the power factor at the rated speed $cos\varphi_{b\infty}$ turns to be constant, such that:

$$cos\varphi_{b\infty} = \frac{1}{\sqrt{2}} \simeq 0.707$$

Comparing the features of the real design and those of the proposed one, under rated armature current operation, it is to be noted that an optimal flux weakening could be fulfilled by:

- 33 percent increase of the armature inductance;
- 12 percent decrease of the constant electromagnetic torque range; and
- 12 percent decrease of the power factor at the base speed.

4. Attempt to improve the EDU cost effectiveness and compactness

In recent years, many research teams worldwide are deeply involved in R&D projects focused towards the design of efficient, cost-effective, compact and reliable HPS in an attempt to reach powertrains which are competitive with ICE-based ones. Of particular interest is the EDU whose design and feature optimization, under standard propulsion cycles, are the subject of intensive investigations. The most important targeted features are:

(1) A high-power density of the electric motor. To this end, new CFMs are under investigation, where many conventional design considerations are rethought, such as the number of phases, the winding shape and distribution, the magnetic circuit geometry and material yielding radial, axial, or transverse flux paths and so on (Zhu, 2009; Ben Hamadou *et al.*, 2009; Tajima *et al.*, 2002).

(2) A high flexibility in the energy management through the propulsion system, in order to access efficient operation cycles (Boldea, 2010; Miller, 2006; Toyota, 2003).

(3) An improvement of the cost effectiveness, the compactness and the reliability, which could be gained through:
   - sensorless control strategies of the electric drive with the elimination of the encoder (Lin *et al.*, 2008; Su and McKeever, 2004); and
   - reduced-structure inverters feeding the electric motor (Elantably *et al.*, 2010; Ben Rhouma and Masmoudi, 2008; El Badsi and Masmoudi, 2008; Ben Rhouma *et al.*, 2007; Lee *et al.*, 2003).

Within the last item, this section is aimed at the operation analysis and the control of a reduced-structure inverter fed brushless DC motor (BDCM) drive. The choice of the BDCM is far from being arbitrary. It is motivated by the low cost of the coupled encoder. The inverter is made up of three legs including each the third of the battery

pack DC bus voltage in series with just one power switch. The yielded legs are delta connected with the summits linked to the BDCM phases, leading to the so-called: "three-switch inverter" (TSI), or "delta-inverter".

4.1 Basis of the delta-inverter-fed BDCM drive

The features of the delta-inverter have been investigated since the beginning of the 80th by Evans *et al.* (1980). They treated the case of delta-connected passive loads, as well as the association with an induction motor under the control of a pre-calculated pulse width modulation strategy.

However, the investigation of the potentialities of the delta-inverter-fed three-phase BDCM drive, for possible integration in HPS, has been considered quite recently by Elantably *et al.* (2010) and Ben Rhouma *et al.* (2007). The connections of such a drive are shown in Figure 7. One can notice that the DC bus is split into three sections which is feasible thanks to the availability of the battery pack.

An improvement of the cost effectiveness could be gained thanks to the integration of the delta-inverter in the EDU. Besides the cost benefit, it leads to an improved compactness. Finally, it reduces the lack of failures of the inverter and therefore improves the drive reliability.

In what follows, the Toyota Prius conventional inverter-fed brushless AC motor (BACM) drive is assumed to be substituted by a delta-inverter-fed BDCM drive. Let us recall the BDCM phase currents and back-EMFs which, under maximum torque production, present the profiles shown in Figure 8.

The 120-electrical degree rectangular-shaped phase currents are controlled by bang-bang regulators. Accounting for the upper and lower limits of these regulators, one can distinguish two sub-sequences for each of the six operating sequences of the BDCM, such that:

(1) an active sub-sequence Seq_i^a during which the power flows from the battery to the BDCM; and

(2) a regenerative sub-sequence Seq_i^r during which the power flows from the BDCM to the battery.

The active and regenerative sub-sequences of the delta inverter-fed BDCM drive are shown in Figure 9.

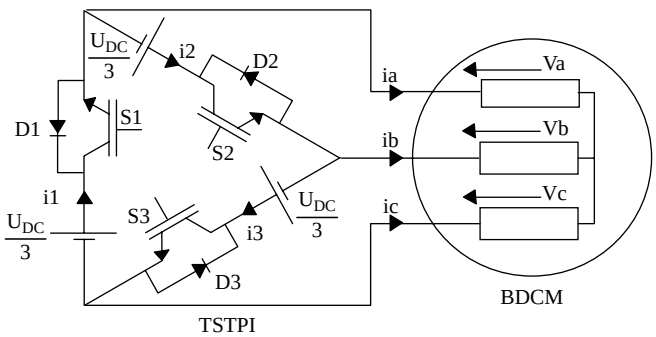

Figure 7.
Connections of the TSI-fed three-phase BDCM drive

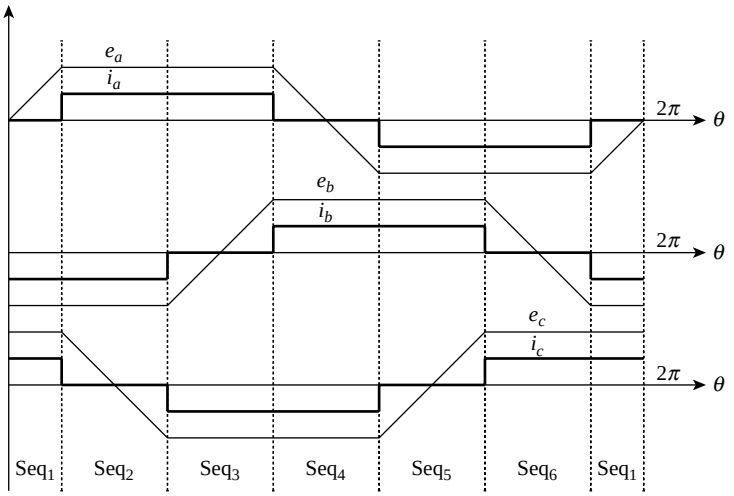

Figure 8.
BDCM phase currents and back-EMFs under maximum torque production

4.2 Delta-inverter-fed BDCM drive: operation characterization

Table I characterizes each sub-sequence $Seq_i^{(a/r)}$ by the involved switches as well as the corresponding phase voltages.

During sequence-to-sequence commutations, two switches (two insulated gate bibolar transistors (IGBTs), two diodes, or an IGBT and a diode) are turned ON, so that the current rises/falls in the two phases under commutation, while it varies between the current regulator limits in the third one.

In the manner of the sequences, the commutations $Com_{i \Rightarrow j}$ from sequence i to sequence j are made up of two sub-commutations each, such that:

(1) $Com_{i \Rightarrow j}^{a}$ when the current rises in the phase not involved in the commutation.

(2) $Com_{i \Rightarrow j}^{r}$ when the current falls in the phase not involved in the commutation.

Table II characterizes each sub-commutation $Com_{i \Rightarrow j}^{(a/r)}$ by the involved switches as well as the corresponding phase voltages.

4.3 Delta-inverter-fed BDCM drive: a dedicated control strategy

Referring to Elantably *et al.* (2010), a dedicated control strategy has been implemented in the delta-inverter-fed BDCM drive. Compared to the one considered for the control of conventional inverter-fed BDCM drives, the scheme includes a torque loop which has been implemented in an attempt to discard the excessive torque ripple during commutations $Com_{i \Rightarrow j}$. The bloc diagram of the control scheme is shown in Figure 10 (Elantably *et al.*, 2010).

4.4 Delta-inverter: battery-pack recharging

A crucial requirement needs to be fulfilled by the delta-inverter topology in order to be integrated in propulsion applications. It concerns its capability of recharging the battery pack. This could be achieved considering the circuit shown in Figure 11.

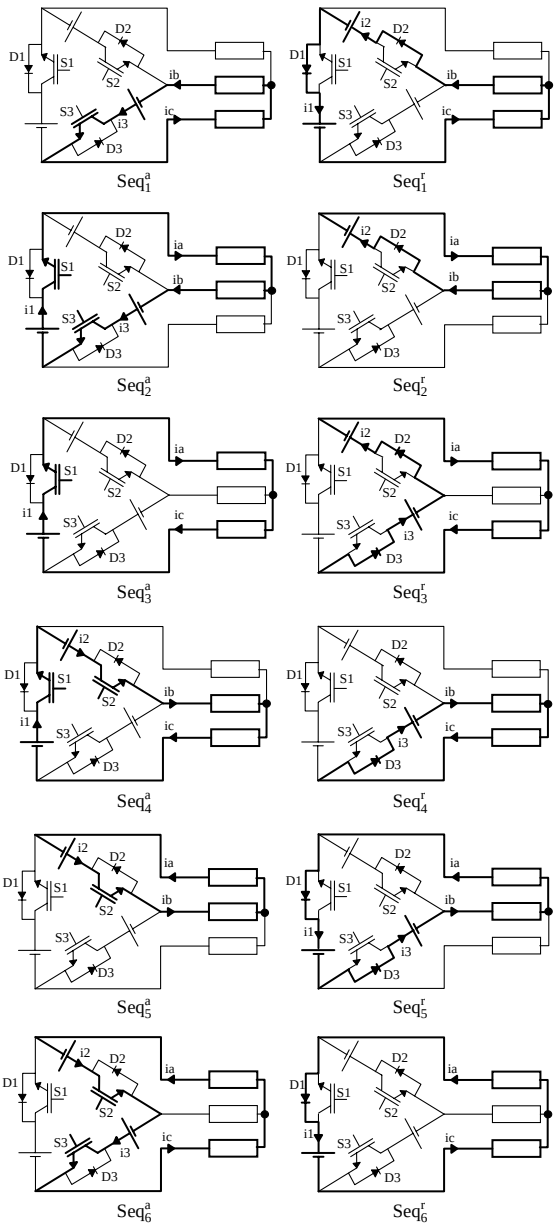

Note: Bold lines indicate the conducting circuits
Source: Ben Rhouma *et al.* (2007)

Figure 9.
The active (left) and regenerative (right) sub-sequences of the TSTPI-fed BDCM drive

Sub-sequence	Conducting switch(es)	Phase voltages V_a	V_b	V_c
Seq_1^a	S3	0	$-U_{DC}/6$	$U_{DC}/6$
Seq_1^r	D1 and D2	0	$U_{DC}/3$	$-U_{DC}/3$
Seq_2^a	S1 and S3	$U_{DC}/3$	$-U_{DC}/3$	0
Seq_2^r	D2	$-U_{DC}/6$	$U_{DC}/6$	0
Seq_3^a	S1	$U_{DC}/6$	0	$-U_{DC}/6$
Seq_3^r	D2 and D3	$-U_{DC}/3$	0	$U_{DC}/3$
Seq_4^a	S1 and S2	0	$U_{DC}/3$	$-U_{DC}/3$
Seq_4^r	D3	0	$-U_{DC}/6$	$U_{DC}/6$
Seq_5^a	S2	$-U_{DC}/6$	$U_{DC}/6$	0
Seq_5^r	D1 and D3	$U_{DC}/3$	$-U_{DC}/3$	0
Seq_6^a	S2 and S3	$-U_{DC}/3$	0	$U_{DC}/3$
Seq_6^r	D1	$U_{DC}/6$	0	$-U_{DC}/6$

Table I.
Characterization of the operating sub-sequences of the delta-inverter-fed BDCM drive

Sub-commutation	Conducting switches	Phase voltages V_a	V_b	V_c
$Com_{1\Rightarrow2}^a$	S1 and S3	$U_{DC}/3$	$-U_{DC}/3$	0
$Com_{1\Rightarrow2}^r$	D1 and D2	0	$U_{DC}/3$	$-U_{DC}/3$
$Com_{2\Rightarrow3}^{(a,r)}$	S1 and D2	0	$U_{DC}/3$	$-U_{DC}/3$
$Com_{3\Rightarrow4}^a$	S1 and S2	0	$U_{DC}/3$	$-U_{DC}/3$
$Com_{3\Rightarrow4}^r$	D2 and D3	$-U_{DC}/3$	0	$U_{DC}/3$
$Com_{4\Rightarrow5}^{(a,r)}$	S2 and D3	$-U_{DC}/3$	0	$U_{DC}/3$
$Com_{5\Rightarrow6}^a$	S2 and S3	$-U_{DC}/3$	0	$U_{DC}/3$
$Com_{5\Rightarrow6}^r$	D1 and D3	$U_{DC}/3$	$-U_{DC}/3$	0
$Com_{6\Rightarrow1}^{(a,r)}$	S3 and D1	$U_{DC}/3$	$-U_{DC}/3$	0

Table II.
Characterization of the sequence-to-sequence sub-commutations of the delta-inverter-fed BDCM drive

One can notice that, during the battery-pack recharging, the BDCM is disconnected from the delta-inverter while the output of the charger is connected in series with the inverter legs so that the charge current flows through diodes D1-D3.

Moreover, it is to be noted that the battery-pack charger could be fed either by:

(1) The starter/alternator when the vehicle is temporarily stopped in locations faraway from the grid (for instance, during refreshment-breaks in highways).

(2) The grid through a plug-in connection (for instance in the garage during the night). It is to be noted that standard charging uses a charging power of 3.3 kW, corresponding to a socket outlet of 230 V, 16 A. This type of charger is the most popular in Europe. It is a single phase AC charger which is dedicated to a normal charging of 6-8 h (Bauer *et al.*, 2010).

4.5 Delta- and conventional inverter-fed BDCM drives: a comparison

This section is devoted to a comparative study between the delta and conventional inverter-fed BDCM drives under steady-state operation. Table III summarizes the features under comparison and the corresponding results.

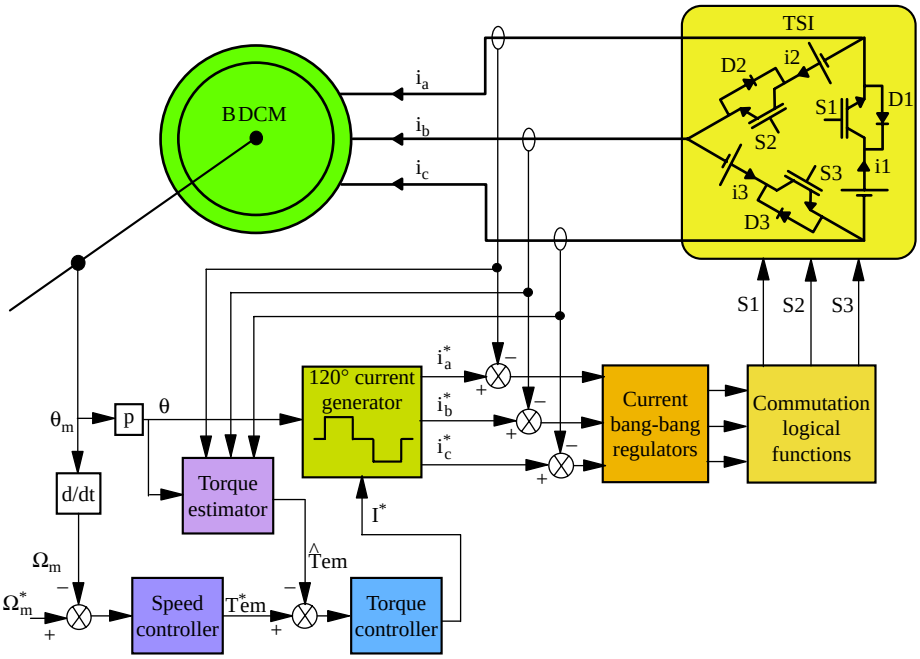

Figure 10.
Bloc diagram of the control strategy implemented in a delta-inverter-fed BDCM drive

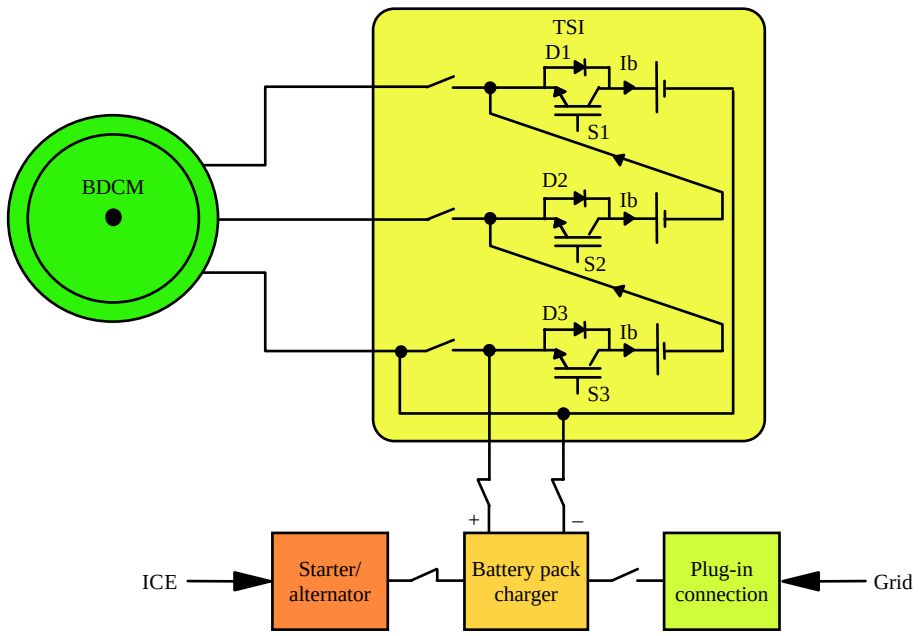

Figure 11.
Circuit dedicated to recharging the battery pack through the diodes of the delta-inverter

Feature under comparison	Conventional inverter	Delta-inverter
α = (number of switches/conventional number of switches)	1	1/2
IGBT minimum rated voltage	U_{DC}	U_{DC}
β = (IGBT minimum rated current/BDCM rated current I)	1	1
Total installed VA of IGBTs	$6\,U_{DC}I$	$3\,U_{DC}I$
BDCM maximum absorbed power P_{max}	$U_{DC}I$	$2/3\,U_{DC}I$
BDCM minimum absorbed power P_{min}	$U_{DC}I$	$1/3\,U_{DC}I$
BDCM average absorbed power P_a	$U_{DC}I$	$1/2\,U_{DC}I$
δ = (Total installed VA of IGBTs/BDCM mean absorbed power)	6	6
γ = (BDCM mean absorbed power/α)	$U_{DC}I$	$U_{DC}I$

Table III.
Comparison between the delta and the conventional inverter fed BDCM drives

From the analysis of these results, one can notice that both drives exhibit the same values of ratios δ and γ, with a 50 percent reduction of the total installed VA of the IGBTs in favor of the delta-inverter, which represents a crucial cost benefit.

5. Conclusion

This paper was devoted to a real illustration-aided initiation of post-graduate students to the basis of HPS. Following a review of the major topologies of HPS; series/parallel hybrid powertrains have been focused considering the Toyota Prius as a case study. A special attention has been paid to the analysis of its major operating cycles.

Assuming that the EDU of the Toyota Prius is equipped by a smooth airgap brushless AC motor with a negligible resistance in the armature, a simple assessment of the features characterizing its flux-weakening operation has been proposed. Then, and within the stimulation of the innovative potentialities of the students, an approach to extend the flux-weakening range through an increase of the motor inductance has been developed. It has been found that an optimal flux weakening could be achieved with 33 percent increase of the armature inductance and with 12 percent decrease of the constant torque range at rated current.

The stimulation of the student innovative potentialities has been reconsidered within the proposal and the analysis of an alternative to improve the cost effectiveness and the compactness of the EDU. It consisted in the substitution of the conventional inverter-fed BACM drive by a delta-inverter-fed BDCM drive. Such a viable candidate has been made feasible thanks to the possibility of splitting the battery pack in three equal parts. A comparison of the steady-state features of both drives has revealed, while the total VA of the IGBTs and consequently the cost of the inverter have been reduced by 50 percent, a decrease with the same ratio has affected the motor average absorbed power, and then its output power.

References

Bauer, P., Zhou, Y., Doppler, J. and Stembridge, N. (2010), "Charging of electric vehicles and impact on the grid: a case study", *Proceedings of the Fifth International Conference and Exhibition on Ecologic Vehicles and Renewable Energies, Monaco*.

Ben Hamadou, G., Masmoudi, A., Abdennadher, I. and Masmoudi, A. (2009), "On the design of a single stator dual rotor permanent magnet machine", *IEEE Trans. on Magnetics*, Vol. 45 No. 1, pp. 127-32.

Ben Rhouma, A. and Masmoudi, A. (2008), "A DTC strategy dedicated to three-switch three-phase inverter-fed induction motor drives", *International Journal for Computation and Mathematics in Electrical and Electronic Engineering COMPEL*, Vol. 27 No. 5, pp. 1098-109.

Ben Rhouma, A., Masmoudi, A. and Elantably, A. (2007), "On the analysis and control of a three-switch three-phase inverter-fed brushless DC drive", *International Journal for Computation and Mathematics in Electrical and Electronic Engineering COMPEL*, Vol. 26 No. 1, pp. 183-200.

Bianchi, N. and Bolognani, S. (2002), "Design techniques for reducing the cogging torque in surface-mounted PM motors", *IEEE Transactions on Industry Applications*, Vol. 38 No. 2, pp. 1259-65.

Bianchi, N., Dai Pre, M., Grezzani, G. and Bolognani, S. (2005), "Design considerations on fractional-slot fault-tolerant synchronous motors", *Proceedings of the IEEE International Electrical Machines and Drives Conference* (*IEMDC*), *San Antonio, TX*, pp. 902-9.

Boldea, I. (2010), "Electric propulsion systems on HEVs: review and perspective", *Proceedings of the Fifth International Conference and Exhibition on Ecologic Vehicles and Renewable Energies, Monaco*.

Elantably, A., Ben Rhouma, A., Masmoudi, A. and Holmes, A.G. (2010), "Control device for driving a brushless DC motor", US Patent 7643733.

El Badsi, B. and Masmoudi, A. (2008), "DTC of a FSTPI-fed induction motor drive with extended speed range", *International Journal for Computation and Mathematics in Electrical and Electronic Engineering COMPEL*, Vol. 27 No. 5, pp. 1110-27.

El-Refaie, A.M. and Jahns, T.M. (2005), "Optimal flux weakening in surface PM machines using concentrated windings", *IEEE Transactions on Industry Applications*, Vol. 41 No. 3, pp. 790-800.

El-Refaie, A.M., Jahns, T.M., McCleer, P.J. and McKeever, J.W. (2006), "Experimental verification of optimal flux weakening in surface PM machines using concentrated windings", *IEEE Transactions on Industry Applications*, Vol. 42 No. 2, pp. 443-53.

Evans, P.D., Dodson, R.C. and Eastham, J.F. (1980), "Delta inverter", *IEE Proceedings B*, Vol. 127 No. 6, pp. 333-40.

Lee, B.K., Kim, T.H. and Ehsani, M. (2003), "On the feasibility of four-switch three-phase BLDC motor drives for low commercial applications: topology and control", *IEEE Transactions on Power Electronics*, Vol. 18 No. 1, pp. 164-72.

Lin, C.T., Hung, C.W. and Liu, C.W. (2008), "Sensorless control for four-switch, three-phase brushless DC motor drive", *IEEE Transactions on Power Electronics*, Vol. 23 No. 1, pp. 438-44.

Miller, J.M. (2006), "HEV propulsion system architectures of the e-CVT type", *IEEE Transactions on Power Electronics*, Vol. 21 No. 3, pp. 756-67.

Su, G.J. and McKeever, W. (2004), "Low-cost sensorless control of brushless DC motors with improved speed range", *IEEE Transactions on Power Electronics*, Vol. 19 No. 2, pp. 296-302.

Tajima, F., Kaizumi, O., Matsunobe, Y., Shibukawa, S., Kawamata, S. and Keiji, O. (2002), "Permanent magnet rotating electric machine and electrically driven vehicle employing same", US Patent 6396183.

Toyota (2003), "Hybrid synergy drive: Toyota hybrid system THS II", available at: www.toyota.co.jpentechenvironmentths2SpecialReports_12.pdf

Zhu, Z.Q. (2009), "Fractional slot permanent magnet brushless machines and drives for electric and hybrid propulsion systems", *Proceedings of the Fourth International Conference and Exhibition on Ecologic Vehicles and Renewable Energies, Monaco*.

About the authors

Asma Ben Rhouma received the BS degree in Electromechanical Engineering in 2004, the MS degree in Machine Analysis and Control in 2005 and the PhD in Electrical Engineering in 2010, all from the Sfax Engineering School (SES), University of Sfax, Tunisia. Asma Ben Rhouma is currently an Associate Professor at the Faculty of Science of Sfax. She is preparing the Research Management Ability degree (HDR) in Electrical Engineering. She is a member of the Research Unit on Renewable Energies and Electric Vehicles (RELEV). She is a member of the Organizing Committee of the International Conference and Exhibition on Ecological Vehicles and Renewable Energies, held every year in Monaco, since 2006. She is a member of the Organizing Committee of the International Workshop on Electric and Hybrid Automotive Technologies: a biannual workshop organized and supported by the RELEV. Asma Ben Rhouma is the inventor of an US patent and the author of many journal and conference papers. Developed within the preparation of her HDR, the major interests of Asma Ben Rhouma are aimed at the design and the control of reduced-structure inverter-fed electrical motor drives and generators, applied in automotive as well as in renewable energy systems.

Ahmed Masmoudi received the BS degree from Sfax SES, University of Sfax, Tunisia, in 1984, the PhD from Pierre and Marie Curie University, Paris, France, in 1994, and the Research Management Ability degree from SES, in 2001, all in Electrical Engineering. In 1988, he joined the Tunisian University where he held different positions involved in both education and research activities. He is currently a Professor of Electric Power Engineering at SES. Ahmed Masmoudi is the Manager of the RELEV. He has been an Associate Researcher with Allison Transmission Division of General Motors, Indianapolis, Indiana, USA. He is the Chairman of the International Conference on Power Electrical Systems organized within the International Multi-conference on Systems, Signals and Devices. He is the Chairman of the Program Committee of the International Conference and Exhibition on Ecological Vehicles and Renewable Energies. He is the Chairman of the International Workshop on Electric and Hybrid Automotive Technologies. He is a member of the International Steering Committee of the Electric Vehicle Symposiums. He is the Editor-in-Chief of the *Transactions on Systems, Signals and Devices*, *Issues on Power Electrical Systems*, published by Shaker-Verlag, Germany. He is a member of the Editorial Board of the international journal *Electromotion*, published by Mediamira Science, Romania. He is a senior member of IEEE. He is the Representative of Africa in the European Association for Battery, Hybrid and Fuel Cell Electric Vehicles. He is a member of the Society of Automotive Engineers, Philadelphia, Pennsylvania, USA. His main interests are focused towards the design of new topologies of electrical machines and the implementation of advanced, efficient and robust control strategies in electrical machine drives and generators, applied in automotive as well as in renewable energy systems. Ahmed Masmoudi is the corresponding author and can be contacted at: a.masmoudi@enis.rnu.tn